animals

MDPI

Article

Hydration-Dependent Failure Resistance of Radular Teeth in the Neritid Gastropod *Vittina turrita*

Wencke Krings [1,2,3,4,*] and Stanislav N. Gorb [1]

[1] Department of Functional Morphology and Biomechanics, Zoological Institute, Kiel University, Am Botanischen Garten 1–9, 24118 Kiel, Germany; sgorb@zoologie.uni-kiel.de
[2] Department of Cariology, Endodontology and Periodontology, Leipzig University, Liebigstraße 12, 04103 Leipzig, Germany
[3] Section Mammalogy and Palaeoanthropology, Leibniz Institute for the Analysis of Biodiversity Change, Martin-Luther-King-Platz 3, 20146 Hamburg, Germany
[4] Department of Electron Microscopy, Institute of Cell and Systems Biology of Animals, University of Hamburg, Martin-Luther-King-Platz 3, 20146 Hamburg, Germany
* Correspondence: wencke.krings@uni-hamburg.de

Simple Summary

Snails use a specialized feeding organ, called the radula, which consists of numerous tiny teeth arranged in rows. These teeth perform different tasks during feeding, such as scraping food from surfaces or collecting loosened particles. In this study, we investigated how tooth shape, position, and hydration influence the resistance of radular teeth to breakage in the aquatic neritid snail *Vittina turrita*. We tested 3000 teeth from 30 individuals under dry and rewetted conditions, measuring the force required to break them and the time until failure. The large lateral teeth resisted the highest forces, whereas the slender marginal teeth tolerated lower forces but reached structural failure after longer loading intervals. Rewetting increased breaking forces by approximately 26–30% and delayed failure in all tooth types. It also changed where the teeth broke, particularly in the marginal teeth. These findings demonstrate that water plays an important role in the mechanical performance of radular teeth and that different tooth types are adapted to different tasks within the feeding apparatus.

Abstract

In the molluscan radula, tooth geometry, material properties, membrane flexibility and contact between neighboring teeth influence loading and failure during feeding. In the neritid gastropod *Vittina turrita*, previous work identified distinct functional roles for the teeth within a rhipidoglossan row. Here, we tested lateral tooth I (LTI), lateral tooth II (LTII), and inner (IMT), medial (MMT) and outer marginal teeth (OMT) under dry and rewetted conditions to determine how tooth function and hydration influence breaking force, loading duration (time from onset of a single loading event to first permanent tooth damage) and failure location. Breaking force differed significantly among tooth types and hydration states, with a significant tooth type × hydration interaction. In both conditions, breaking force followed LTII > LTI > IMT > MMT > OMT, and rewetted teeth resisted significantly higher forces than dry teeth. Loading duration increased from LTI to OMT and was longer in rewetted preparations. Failure locations also differed between the two treatments. Rewetted LTI showed localized damage at its bridge-like joint with the central tooth, whereas dry LTI crumbled there. Dry LTII failed at the cusp, while rewetted LTII failed variably at the cusp, stylus or basis. Marginal teeth shifted from cusp failure when dry to basal failure after rewetting. Under these preparation and loading conditions, rewetting increased failure resistance and changed where teeth broke. The patterns are consistent with different modes of load transfer among tooth types, particularly bending of the marginal teeth.

Check for updates

Academic Editor: Rafæl Campos-Ramos

Received: 23 October 2026
Revised: 23 November 2026
Accepted: 27 November 2026
Published: 29 November 2026

Copyright: © 2026 by the authors. Licensee MDPI, Basel, Switzerland. This article is an open access article distributed under the terms and conditions of the Creative Commons Attribution (CC BY) license.

Keywords: radula; structural failure; breaking force; hydration; finite element analysis; functional morphology; biomaterials; Mollusca

1. Introduction

Most molluscs use the radula to collect and process food, repeatedly bringing its teeth into contact with food or the underlying substrate. It consists of serial transverse rows of chitinous teeth embedded in a flexible radular membrane and functions as part of the buccal mass together with odontophoral cartilages and associated musculature [1–3]. Radular action is often described as rasping or scraping, yet work on living animals and experimentally protruded radulae has shown that radular motion is taxon-specific and three-dimensional, involving bending, rotation, folding and changes in tooth orientation during a feeding cycle [4–9]. Kinematic studies of the buccal mass and structural analyses of other gastropods likewise demonstrate that the radula operates as part of an integrated feeding apparatus rather than as a flat conveyor of isolated teeth [10,11]. Teeth must therefore be considered together with their membrane attachment, neighbouring teeth and supporting odontophoral structures.

Radular loading depends on the buccal mass, the arrangement of the tooth rows and the mechanics of individual teeth. Buccal musculature generates force [7,12]; tooth arrangement governs contact and load redistribution [5,9,13,14]; and tooth geometry and attachment govern leverage, bending and force transfer [13,15–18].

The diversity of radular morphology has long been interpreted in the context of trophic ecology. Tooth number, size, aspect ratio, cusp shape and arrangement vary strongly among molluscan taxa and are associated with the type of food processed and the substrate on which it is collected [15,16,19–24]. Broader and more robust teeth are commonly associated with loosening or scraping attached food, whereas slender and pointed teeth can facilitate piercing, cutting, brushing or particle gathering [2,16,25,26]. Experiments and models show that tooth shape alone does not determine function: the feeding configuration, tooth-tooth contacts and local loading direction strongly modify the mechanical role of a given morphology [6,8,9,27].

Tooth material also matters. Radular teeth are biological composites whose mechanical properties differ among tooth types and across regions of the same tooth. In highly mineralized Polyplacophora and Patellogastropoda, iron- and silica-bearing mineral phases, highly organized fiber architectures and graded interfaces generate exceptionally stiff and wear-resistant cutting structures [28–33]. Other molluscan groups possess much lower levels of bulk mineralization but nevertheless show pronounced local differences in Young's modulus and hardness, frequently with harder and stiffer cusps or contact regions and more compliant styli (elongated shaft-like regions supporting the cusps), bases (proximal regions anchoring the teeth to the radular membrane) or supporting regions [34–39]. Young's modulus reflects elastic stiffness and influences deformation and stress distribution within a tooth, whereas hardness reflects resistance to local plastic deformation and is commonly associated with resistance to wear. Neither property alone necessarily predicts the location or load at which structural failure occurs.

Material gradients arise through mineral incorporation, metal-ion cross-linking, tanning, fiber organization and Ca- or Si-rich coatings [37,38,40–46]. Stiff-to-compliant transitions reduce stress concentrations and preserve mobility [47–49], producing functionally graded tools [27,36,39].

During feeding, radular teeth must engage food and substrates while resisting wear and breakage. Radular damage includes scratches, chipping, microcracks, fractures and

spalling [26,50–53]. Fibers and material gradients can redirect damage [32,49,53], while continuous renewal limits the required service life [54,55].

Tooth hardness or stiffness alone cannot explain when the tooth–membrane system fails. Experimental breaking studies on taenioglossan gastropods showed that the load required for failure depends on tooth morphology, material properties, hydration, the size of the attachment to the membrane and the ability of neighboring teeth to support one another [14,56]. Broad, interlocking teeth can transfer load to adjacent rows, whereas long and slender teeth may undergo large bending or twisting amplitudes before failure. Failure was often detected in compliant regions or in parts of a tooth not mechanically supported by neighboring elements, rather than in the hardest cusp itself [14]. Tooth attachment is likewise important: larger attachment areas can distribute stress more broadly, whereas smaller attachments permit greater deflection and mobility [13,14].

Because the radula functions in aquatic environments that may differ in salinity, water content and dissolved ions, these factors may affect the mechanics of both the teeth and their supporting membrane. More generally, interactions with water can influence the structural organization of biological materials. For example, theoretical work on model lipid membranes has demonstrated how hydration and structural reorganization can be coupled processes [57], although the underlying mechanisms differ from those in chitin–protein composites. Water can plasticize water-permeable chitin–protein composites, increasing deformability and often lowering Young's modulus and hardness. In the integrated tooth–membrane system, these material changes may facilitate load redistribution before structural failure [14,30,56]. In paludomid radulae, wet teeth and membranes were more compliant, enabling individual teeth to bend, twist or slip away from obstacles and, in some tooth types, to gain support from adjacent rows. This collective response allowed the hydrated radula to tolerate higher externally applied forces before structural failure even though the local tooth material was less stiff [14,56]. Hydration can therefore affect tooth movement, contact between teeth, and material stiffness.

Finite-element analysis (FEA) provides a complementary way to separate the effects of geometry, stiffness and material distribution. Comparative FEA of taenioglossan teeth has shown that three-dimensional shape, dimensions and assigned Young's modulus values influence stress, strain and deformation under standardized loading [17,18]. Studies of chiton radular structures have similarly demonstrated the mechanical importance of a compliant, fiber-reinforced stylus supporting a more strongly reinforced distal region [49,58]. Such simulations are especially valuable because internal stress and strain fields cannot readily be measured in intact micrometer-scale teeth during loading. However, comparative FEA is most informative when models are interpreted according to their assumptions and experimentally validated; standardized loads are useful for comparing structures but do not by themselves represent physiological forces or predict fracture thresholds [59].

The neritid gastropod *Vittina turrita* (J.F. Gmelin, 1791) has a rhipidoglossan radula that folds during feeding, changing tooth orientation and substrate contact [8]. The species occurs in brackish mangrove and riverine habitats of Southeast Asia, including freshwater reaches [8,60]. Laboratory observations indicate that adults tolerate salinities from freshwater (0 ppt) to seawater (35 ppt), although this range does not encompass the salinity at all natural feeding sites [60]. The snails graze algae on submerged solid surfaces, including rocks and plant material, where substrate characteristics may affect tooth loading and wear [8]. Previous feeding experiments identified different roles for the lateral and marginal teeth, including scraping, radular folding and particle gathering. They also documented progressive damage from scratches to fractures and spalling and indicated functional differentiation from the inner towards the outer marginal field [8]. Nanoindentation revealed differences in stiffness and hardness among *V. turrita* tooth types, with LTII particularly

stiff and hard and local reinforcement in LTI and the inner marginal teeth [61]. Regional differences are associated with tanning, elemental composition and a thin calcium-rich coating [61]. These measurements were performed under dry conditions, although the radula functions wet and hydrated tissues may be more compliant [30,61]. A complementary FEA of *V. turrita* compared mechanical responses of LTI, LTII, IMT and OMT across different modulus assignments [62]. Marginal teeth exhibited substantial stylus deformation and bending-dominated behaviour. Geometry largely determined the response pattern, while stiffness influenced deformation magnitude [62]. The models did not simulate fracture or predict experimental failure forces; MMT was investigated only in the present experiments.

The present study tests structural failure in *V. turrita* under controlled shear loading, asking how tooth type and hydration affect mechanical specialization. LTI, LTII, IMT, MMT and OMT were compared under dry and rewetted conditions using breaking force, loading duration and anatomical failure location. The observations are considered in relation to a separate companion FEA study in the Discussion, solely to provide qualitative biomechanical context.

We tested whether (1) tooth types differ in load-bearing capacity according to their mechanical roles; (2) performance changes systematically across the marginal field; and (3) hydration alters breaking force, loading duration and the anatomical failure pathway, potentially through changes in compliance and load redistribution.

2. Materials and Methods

2.1. Study Species and Experimental Design

Adult specimens of *Vittina turrita* (Gastropoda: Neritidae) were used for breaking force experiments. They were obtained from a pet shop (available online at garnelio.de; here, gastropods are sold as *Neritina turrita*). Species identification was based on shell and operculum morphology after the experiments. Snails were killed by a short boiling (2 s) and then preserved in 70% EtOH. This species possesses a rhipidoglossan radula with one central tooth, two lateral teeth on each side and numerous marginal teeth per transverse row; previous morphometric and feeding analyses are described in Krings et al. [8]. Thirty specimens were investigated, with 15 specimens tested under dry conditions and 15 under wet conditions. For each specimen, 20 teeth were tested for each of five tooth categories: LTI, LTII, IMT, MMT and OMT (see Figure 1), resulting in 3000 individual tooth tests. The three marginal categories represent defined inner, medial and outer regions of the marginal field. Repeated tooth tests within a specimen were treated as within-specimen subsamples, whereas the individual gastropod represented the biological replicate.

2.2. Radula Preparation and Hydration Treatment

Radula preparation was adapted from the experimental failure protocol established previously for gastropod radulae [14,56], but the three-dimensional configuration of the radula of *V. turrita* was preserved. The whole buccal mass was carefully extracted with soft tweezers. Surrounding tissues were trimmed only as required for handling, while the tissue directly underlying and supporting the radula was retained so that the radula remained associated with the buccal mass and maintained its three-dimensional architecture. Preparations were handled at non-functional regions whenever possible to avoid damage to the mature working zone. These radulae were dried with a series of increasing alcohol concentrations (80%, 90%, 100%, 100% EtOH, for 1 h each) and then placed in a 1:1 solution of 100% EtOH and 100% acetone, followed by 100% acetone (for 1 h each). Critical point drying with carbon dioxide was performed with the Leica EM CPD300 (Leica Camera AG, Wetzlar, Germany) at 20 cycles. Residual water content was not measured gravimetrically; thus, 'dry' refers to specimens subjected to solvent dehydration without

subsequent rewetting, not to a verified complete absence of bound water. Teeth used for mechanical testing were selected from fully mature rows of the working zone and remained attached to the radular membrane and supported by the underlying buccal mass, thereby retaining the three-dimensional tooth arrangement, membrane curvature and potential mechanical interactions among neighboring teeth.

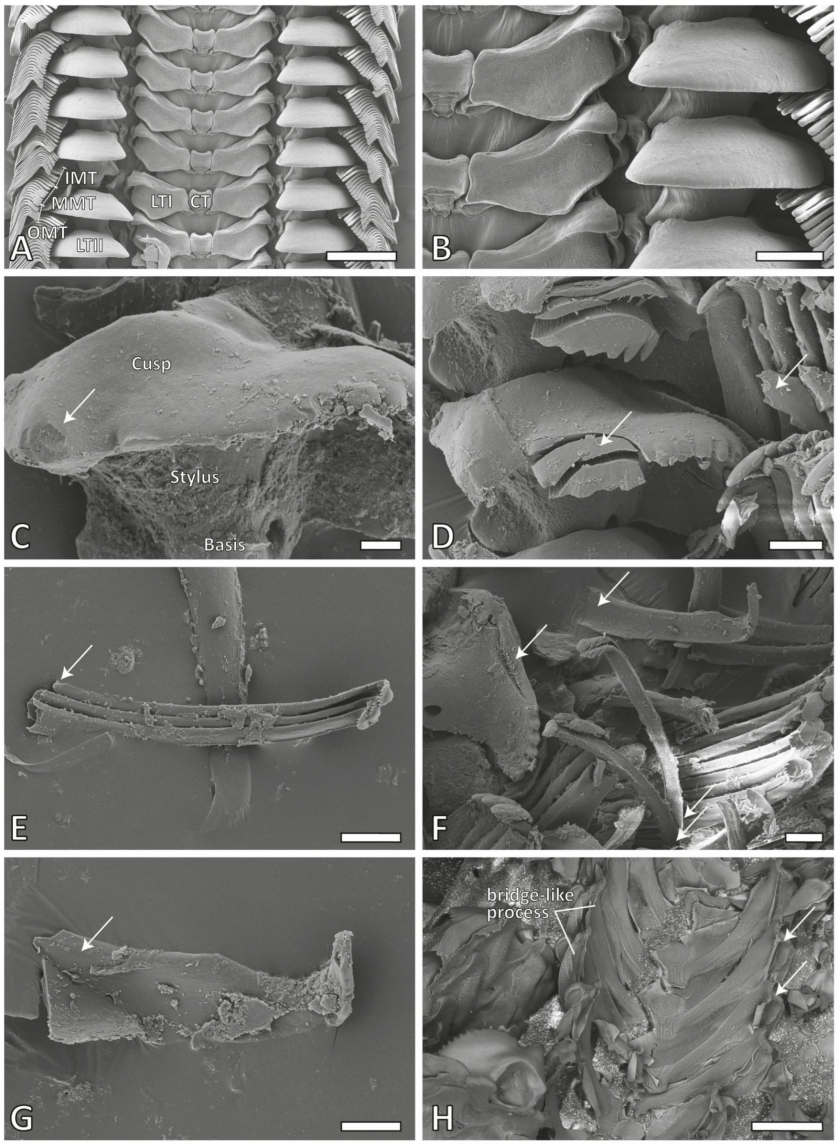


Figure 1. Radular morphology and representative structural failure locations (arrows indicate fracture sites) in *Vittina turrita*. (**A**) SEM overview of the mature unbroken working zone showing the central tooth (CT), lateral tooth I (LTI), lateral tooth II (LTII), and inner (IMT), medial (MMT) and outer marginal teeth (OMT). (**B**) Higher-magnification view illustrating the three-dimensional arrangement and close association of the lateral and marginal teeth. (**C**) Representative LTII showing cusp failure in a dry preparation. (**D**) Representative structural damage to LTII and IMT after testing of a rewetted preparation. (**E**) Structural damage of OMT after wet failure. (**F**) Representative of the LTII and proximal failure of IMT and MMT following extensive bending after wet failure; arrows indicate damaged or fractured regions near the tooth bases. (**G**) Representative damage of IMT after wet failure, with the arrow indicating the affected region. (**H**) View of the LTI–central-tooth region showing the bridge-like process involved in the joint-associated connection; arrows indicate structural damage after wet failure. Abbreviations: IMT, inner marginal teeth; LTI, lateral teeth I; LTII, lateral teeth II; MMT, medial marginal teeth; OMT, outer marginal. Scale bars: (**A**), 200 µm; (**B**), 80 µm; (**C**), 10 µm; (**D**–**G**), 20 µm; (**H**), 100 µm.

The resulting three-dimensional preparation was fixed with the side of the supporting structures to a microscope glass slide with epoxy (RECKLI Epoxy WST, RECKLI GmbH, Herne, Germany), providing a stable attachment without collapsing the radular curvature or tooth-to-tooth relationships. Preparations assigned to the dry condition were tested in this critical-point-dried state. Preparations assigned to the wet condition were rehydrated after fixation by applying distilled water without added salts with a pipette immediately before mechanical testing. Distilled water was used to standardize the rewetting procedure across specimens and facilitate reproducibility by avoiding uncontrolled variation in dissolved ions and other constituents of environmental water. Its use was not intended to reproduce the physicochemical conditions encountered during feeding. Larger water drops, attached to the teeth, were absorbed with paper and thus removed. When radulae became too dry during experiments, wetting was repeated. Because the underlying buccal mass and the three-dimensional radular configuration were retained during solvent treatment, mounting and subsequent rewetting, the experimental setup reproduced the spatial curvature and relative tooth arrangement characteristic of the functional radula described for *V. turrita* [8].

2.3. Breaking Force Experiments

The force-measurement apparatus and shear-loading principle were adapted from the previous radular failure experiments [14,56]. The glass slide carrying the three-dimensionally preserved radula-buccal-mass preparation was positioned under a binocular microscope (see Figure 2). A rounded steel needle with a diameter of 0.4 mm was firmly attached to a FORT-1000 force transducer (World Precision Instruments, Sarasota, FL, USA), connected to an amplifier (BiopacSystem, Inc., Goleta, CA, USA) and a computer-based data acquisition and processing system (AcqKnowledgeTM, version 3.7.0.0, Biopac Systems, Inc., v.3.7.0.0, World Precision Instruments, Sarasota, FL, USA). The needle was positioned on the functional region of a fully mature tooth at an angle of approximately 30° and advanced at a constant nominal speed of 0.05 mm/s using a remote-controlled micromanipulator (DC 3001R, World Precision Instruments Inc., Sarasota, FL, USA), applying shear in the antero-posterior direction until the first irreversible structural failure occurred. Each target tooth underwent a single continuous loading event. The needle was advanced without deliberate pauses or cyclic loading; no independent displacement signal was recorded. Because the radula remained attached to the underlying buccal mass in its preserved three-dimensional configuration, tooth attachment to the radular membrane, radular curvature and, where present, mechanical support from neighboring teeth were retained during loading.

For each successful test, specimen identity, hydration condition, tooth type, tooth position, tooth row position and the force trace were recorded. We recorded two quantitative outcomes. Breaking force was defined as the maximum baseline-corrected force immediately preceding the first irreversible structural failure. Loading duration (time to first structural failure) was defined as the interval from the onset of this single continuous loading event to the first structural failure. Here, "irreversible" denotes permanent tooth damage, such as cracking, fracture or fragmentation, rather than recoverable elastic deflection. The first failure event was assessed from the recorded force trace in conjunction with the observed and post-test damage morphology.

Force recordings were exported from AcqKnowledge in mN. The stable pre-contact segment immediately preceding loading onset was used to determine the baseline, and its mean value was subtracted from the trace before analysis.

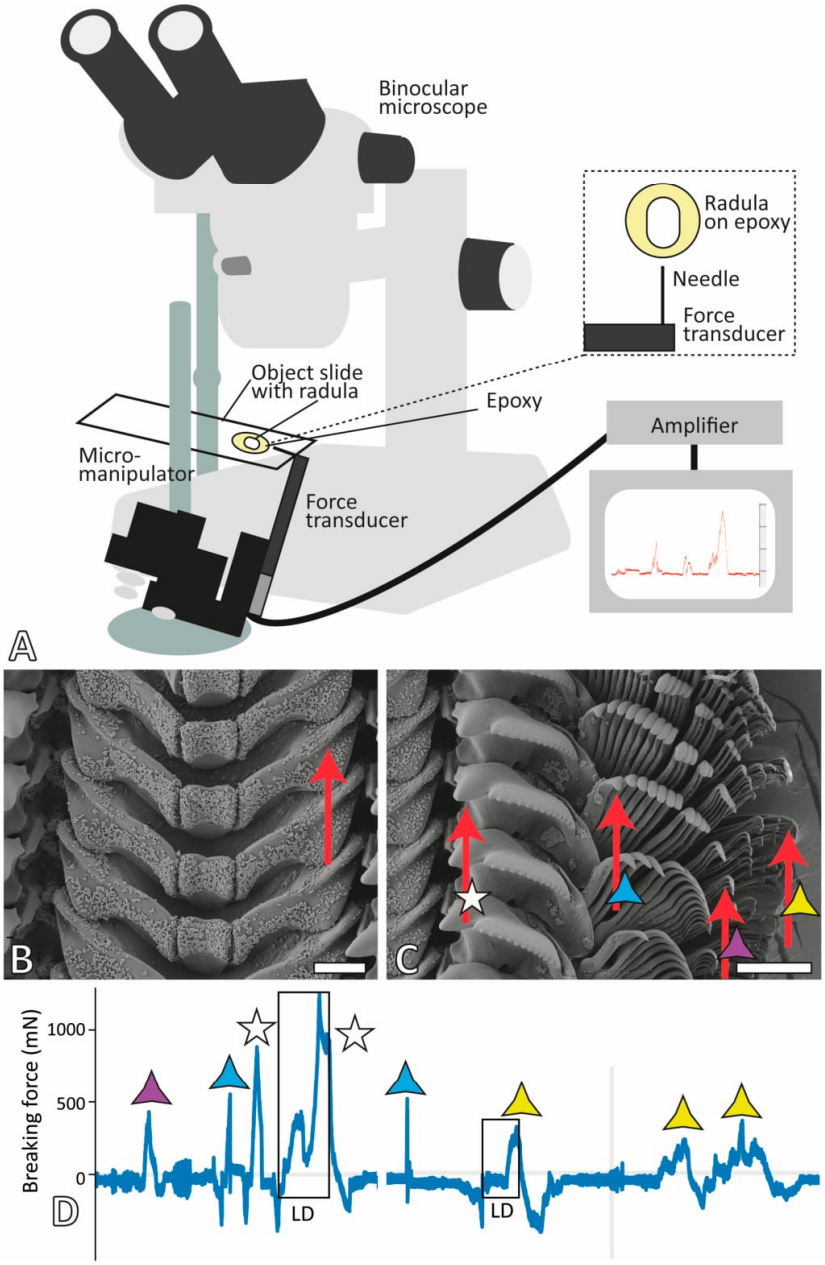


Figure 2. Experimental setup for breaking force measurements of *Vittina turrita* radular teeth. (**A**) Schematic representation of the mechanical testing setup. The three-dimensionally preserved radula–buccal-mass preparation was fixed to a microscope slide with epoxy and positioned under a binocular microscope. A rounded steel needle connected to a force transducer was positioned and advanced using a micromanipulator; the force signal was amplified and continuously recorded. The inset illustrates the relative arrangement of the radula, needle and force transducer during loading. (**B**,**C**) SEM images illustrating the direction of force application to teeth within the mature working zone; red arrows indicate the direction of shear loading. (**D**) Representative baseline-corrected force recording obtained during sequential mechanical loading of radular teeth (stars: LTII; blue triangles: inner marginal teeth; purple triangle: medial marginal tooth; yellow triangles: outer marginal teeth), showing individual loading events and their force peaks; the trace illustrates the force signal, whereas breaking force was extracted for each individual tooth at its first irreversible structural failure. The continuous force trace represents sequential loading of different teeth. Between loading events, the force sensor and attached probe were slightly repositioned to contact the next tooth while recording continued. Each force peak corresponds to a separate loading event. Loading duration (LD) was determined individually for each tooth, excluding the intervals between tests. Scale bars: (**B**), 60 µm; (**C**), 100 µm.

2.4. Failure Mode and Post-Failure Imaging

After mechanical testing, radulae were documented with a SEM Zeiss LEO 1525 (One Zeiss Drive, Thornwood, NY, USA) or Tabletop SEM TM4000 Plus (Hitachi, Tokyo, Japan), following the post-failure imaging approach used in the previous breaking experiments [14]. Failure events were classified according to the damaged structure and anatomical location. For LTI, particular attention was paid to the bridge-like, joint-associated process connecting LTI with the central tooth, previously implicated in folding of the radular row [8]. For LTII and the marginal teeth, failure was scored at the cusp, stylus or basis. Failure morphology was additionally described as a discrete fracture or as diffuse crumbling/fragmentation when no sharply defined fracture plane was visible.

Membrane rupture was recorded separately from primary tooth failure. In some experiments, excessive bending of the loaded tooth resulted in failure of the radular membrane. However, in most cases the first irreversible event was structural failure of the tooth itself. After tooth failure, continued probe movement frequently caused the rounded needle to slide across the damaged tooth and subsequently tear the radular membrane. Such secondary membrane rupture was therefore distinguished from the primary tooth-failure event and was not included as an endpoint in the present analysis. The endpoint was tooth failure, not the ultimate failure of the entire tooth–membrane complex.

2.5. Statistical Analysis

First analyses were carried out in JMP Pro, Version 14 (SAS Institute Inc., Cary, NC, USA, 1989–2007). Individual gastropods were treated as biological replicates. Because 20 teeth of each tooth type were tested per specimen, tooth-level measurements were considered within-specimen subsamples rather than independent biological replicates. For each specimen, we calculated the mean breaking force and mean time to first structural failure for every tooth type. Hydration condition (dry versus wet) was treated as a between-specimen factor, whereas tooth type (lateral teeth I, lateral teeth II, IMT, MMT and OMT) was a repeated within-specimen factor.

Breaking force and time to first structural failure were analysed separately using Gaussian generalized estimating equations (GEE) with specimen identity as the clustering variable and an exchangeable working correlation structure. Models included hydration condition, tooth type and the hydration × tooth type interaction. Type III Wald tests were obtained using sum-to-zero effect coding. Model residuals were evaluated using residual plots and Shapiro–Wilk tests, and homogeneity of variance among tooth type × hydration groups was assessed using Brown-Forsythe tests. Because variance heterogeneity was detected, inferential tests were based on robust sandwich covariance estimates. Following the overall model tests, model-based post hoc contrasts compared wet versus dry conditions separately within each tooth type and all pairwise differences among tooth types separately within the dry and wet conditions. *p*-values were adjusted for multiple comparisons using the Holm procedure. All tests were two-sided and statistical significance was accepted at alpha = 0.05. Quantitative analyses were performed in Python 3.13.5 using statsmodels 0.14.6; distributional tests were performed with SciPy 1.17.0. Failure-location and failure-morphology patterns were treated descriptively because systematic event counts were not available for categorical modelling.

3. Results

3.1. Breaking Force

The dataset (see Figure 3, Tables S1 and S2) comprised 30 specimens, with 15 specimens per hydration condition and 20 tooth tests per tooth type and specimen, yielding 300 measurements for each tooth type × hydration combination and 3000 tooth tests in

total. Model residuals showed no significant departure from normality for breaking force (Shapiro–Wilk W = 0.988, $p = 0.206$), whereas variance differed among tooth type × hydration groups (Brown-Forsythe F = 3.19, $p = 0.0015$); consequently, inference was based on robust covariance estimates (Table S3). Breaking force was significantly affected by hydration (Wald $\chi^2 = 243.66$, df = 1, $p < 0.0001$), tooth type (Wald $\chi^2 = 7849.16$, df = 4, $p < 0.0001$) and their interaction (Wald $\chi^2 = 85.94$, df = 4, $p < 0.0001$; Table S4). In both hydration conditions, breaking force followed the same rank order, LTII > LTI > IMT> MMT > OMT. Specimen-level means and standard deviations for both hydration conditions are provided in Tables S1 and S2. The full set of individual tooth measurements is provided as Supplementary Data S1 (Excel workbook).

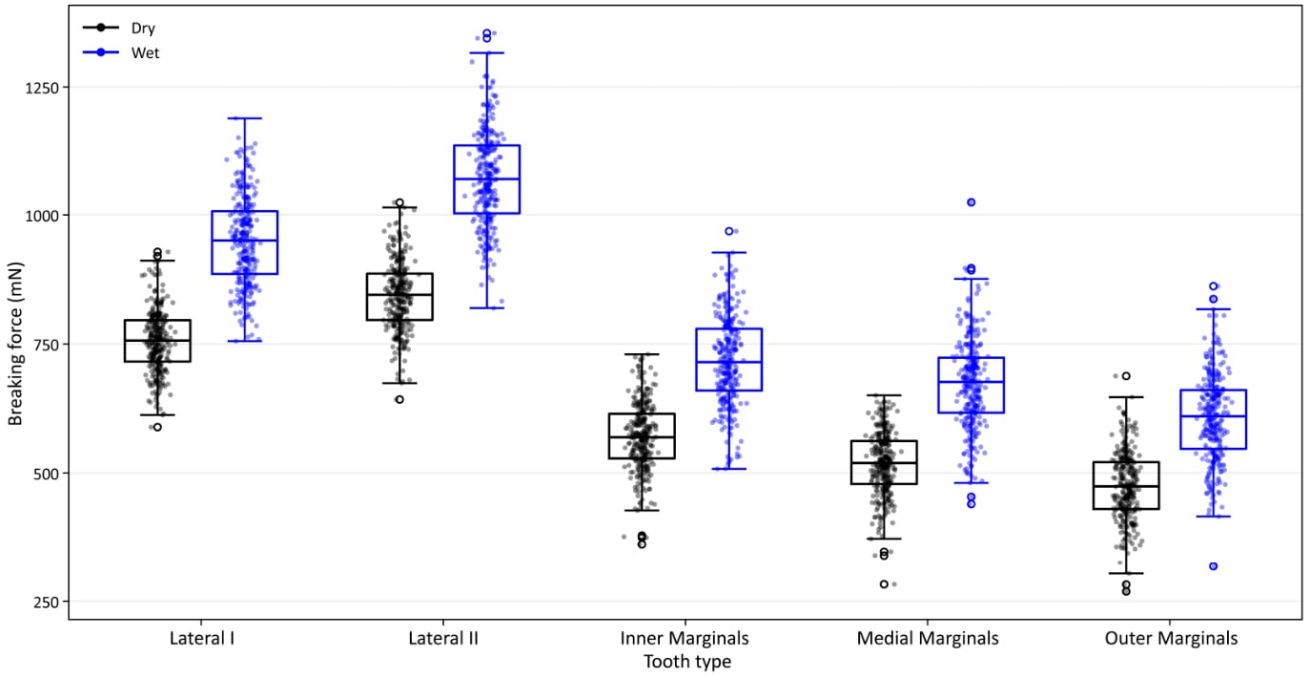


Figure 3. Breaking force of radular tooth types of *Vittina turrita* under dry and wet conditions. Breaking force (mN) is shown for lateral tooth I, lateral tooth II, inner marginal teeth, medial marginal teeth and outer marginal teeth. Dry preparations are shown in black and wet preparations in blue. Each point represents an individual tooth measurement (300 teeth per tooth type and treatment: 15 biological replicates per treatment, with 20 subsampled teeth per tooth type and specimen). Statistical models were fitted to specimen-level means rather than treating teeth as independent biological replicates. Boxes indicate the interquartile range with the median, whiskers extend to 1.5× the interquartile range, and open circles indicate values beyond the whiskers. Breaking force was higher under wet than dry conditions for all tooth types and decreased from lateral tooth II towards the outer marginal field.

Model-based hydration contrasts showed higher breaking forces under wet than dry conditions for each tooth type (all Holm-adjusted $p < 0.0001$; Table S5). The estimated wet-dry differences were +193.66 mN for LTI, +228.11 mN for LTII, +148.05 mN for IMT, +153.39 mN for MMT and +132.45 mN for OMT. Expressed relative to the corresponding dry means, these increases were 25.6% for LTI, 27.0% for LTII, 26.0% for IMT, 29.6% for MMT and 27.9% for OMT (approximately 26–30% across tooth types). The proportional changes were therefore broadly similar despite substantial differences in absolute load-bearing capacity. Pairwise post hoc comparisons among tooth types were also significant within both dry and wet conditions (all Holm-adjusted $p < 0.0001$; Table S6), statistically separating the two lateral teeth from one another and from the progressively lower-force marginal positions. Thus, hydration increased failure resistance across the complete tooth row while preserving a pronounced tooth-type-specific hierarchy in load-bearing capacity.

3.2. Time to First Structural Failure

Model residuals for time to first structural failure (see Figure 4, Tables S1 and S2) showed no significant departure from normality (Shapiro–Wilk W = 0.986, $p = 0.148$), whereas group variances were heterogeneous (Brown-Forsythe F = 4.62, $p < 0.0001$; Table S3). Robust GEE analysis showed significant effects of hydration (Wald $\chi^2 = 229.28$, df = 1, $p < 0.0001$), tooth type (Wald $\chi^2 = 10{,}099.04$, df = 4, $p < 0.0001$) and the hydration × tooth type interaction (Wald $\chi^2 = 31.95$, df = 4, $p = 0.000002$; Table S4). In contrast to breaking force, time to first structural failure increased from the lateral teeth towards progressively more lateral marginal positions. Specimen-level means and standard deviations for both hydration conditions are provided in Tables S1 and S2.

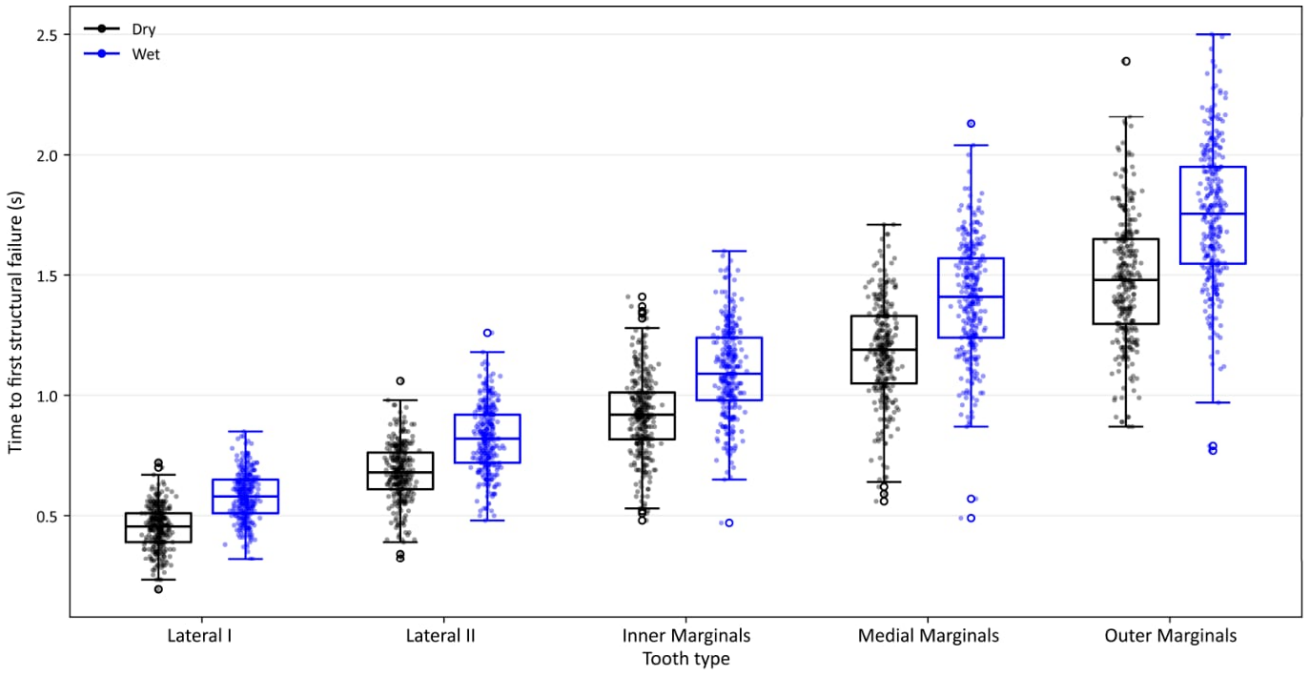


Figure 4. Time to first structural failure of radular tooth types of *Vittina turrita* under dry and wet conditions. Time from loading onset to first irreversible structural failure (s) is shown for lateral tooth I, lateral tooth II, inner marginal teeth, medial marginal teeth and outer marginal teeth. Dry preparations are shown in black and wet preparations in blue. Each point represents an individual tooth measurement (300 teeth per tooth type and treatment: 15 biological replicates per treatment, with 20 subsampled teeth per tooth type and specimen). Statistical models were fitted to specimen-level means rather than treating teeth as independent biological replicates. Boxes indicate the interquartile range with the median, whiskers extend to 1.5× the interquartile range, and open circles indicate values beyond the whiskers. Time to first structural failure increased from the lateral teeth towards the outer marginal field and was longer under wet than dry conditions.

Wet teeth reached first structural failure significantly later than dry teeth for each tooth type (all Holm-adjusted $p < 0.0001$; Table S5). The estimated wet-dry increases were 0.130 s for LTI, 0.140 s for LTII, 0.180 s for IMT, 0.220 s for MMT and 0.270 s for OMT. All pairwise tooth-type contrasts were significant within both hydration conditions (all Holm-adjusted $p < 0.0001$; Table S6), yielding the inverse positional sequence LTI < LTII < IMT< MMT < OMT. The increasing hydration effect towards the outer marginal field indicates that the duration of loading before first structural failure is particularly sensitive to hydration in the more compliant marginal teeth. At the constant nominal probe speed of 0.05 mm/s, these wet–dry differences correspond to 6.5–13.5 µm of additional nominal probe travel. However, no independent displacement of the tooth or membrane was recorded.

3.3. Failure Modes and Locations

Qualitative inspection revealed distinct tooth-type- and hydration-dependent failure patterns (Figure 1; Table S7). In wet LTI, damage was small and localized at the bridge-like process connecting LTI with the central tooth, while the main tooth body remained comparatively intact. Dry LTI failed in the same bridge region, but the affected material lacked a clearly defined fracture surface and instead crumbled or fragmented. Dry LTII failed at the cusp, whereas wet LTII showed no single consistent failure location, with damage observed at the cusp, stylus or basis. The marginal teeth showed the clearest hydration-dependent shift: inner, medial and OMT failed at the cusp under dry conditions but at the tooth basis under wet conditions.

Failure-location and failure-morphology frequencies have not yet been systematically scored; these observations are therefore reported qualitatively and are not included in the inferential statistical analyses presented above.

4. Discussion

The present study extends the structure-function framework for *Vittina turrita* radula from feeding kinematics and material differentiation to experimentally measured structural failure. Previous work established the three-dimensional feeding configuration and tooth-specific substrate contact [8], identified strong spatial heterogeneity in Young's modulus, hardness, composition and surface reinforcement [61], and predicted geometry-dependent stress and strain responses by FEA [62]. The present results add two central functional findings. First, breaking force and loading duration differ systematically among tooth types, confirming mechanical differentiation across the radular row. Second, hydration affects both variables in a tooth-type-specific manner and changes the anatomical route to failure. This distinction matters because the radula normally operates in water, whereas the material-property measurements used to parameterize the FEA were obtained under dry conditions. Nevertheless, rewetting specimens after solvent dehydration and critical-point drying with distilled water does not reproduce the native hydrated condition (see Section 4.6).

4.1. Breaking Force in the Context of Radular Biomechanics

Breaking force measures structural failure under an imposed load; it is neither the force generated during feeding nor an intrinsic material strength. In vivo studies have quantified gastropod radular forces during feeding and shown that force performance scales with body mass, but these measurements represent forces generated by the buccal apparatus under behavioural conditions rather than the maximum load a single tooth can withstand [7,12]. For example, in *Cornu aspersum*, anterior scratching forces averaged 31.57 ± 19.23 mN and reached 106.91 mN [7]; across three body-mass classes of stylommatophoran gastropods, mean absolute feeding forces ranged from 14.46 to 73.96 mN [12]. These in vivo measurements reflect forces from the interacting feeding apparatus and cannot be used directly to infer the normal load or safety factor of a single *V. turrita* tooth. In the present experiments, the external load was increased until a tooth failed. In paludomid gastropods, experimentally measured failure forces were much higher than force values estimated for normal feeding, suggesting substantial structural safety margins, although absolute values cannot be transferred directly between taxa with different radular designs [14]. The present *V. turrita* values, spanning approximately 0.48–1.07 N across tooth types and hydration states, therefore fall within the same broad order of magnitude as failure forces reported for other gastropod radular systems, while remaining directly comparable only within the present standardized protocol.

4.2. Functional Division of Labor Among Lateral and Marginal Teeth

Breaking force separated all five tooth types and followed the same hierarchy under dry and wet conditions (LTII > LTI > IMT> MMT > OMT), while the significant hydration × tooth type interaction showed that hydration did not influence all tooth types identically. This ranking is consistent with differences in tooth function. Broad, compact lateral teeth (LTI and LTII) are mechanically suited to retain shape and transmit localized forces, whereas slender marginal teeth (IMT, MMT and OMT) can bend, twist or conform to irregular surfaces [2,15,16,20]. These different tooth shapes occur within the same transverse row: resistance to high force is advantageous for a scraping or loosening tooth, whereas controlled deformation is advantageous for a sweeping, conforming or gathering tooth [5,27].

Previous feeding experiments help explain these differences among the teeth. LTII is the most obvious load-bearing scraper: its cusp produces the clearest feeding tracks, it experiences pronounced substrate exposure and it has the highest local Young's modulus and hardness values [8,61,63]. LTI is mechanically more complex. Its lateral region interacts with the substrate, but its medial bridge-like connection to the central tooth participates in the folding mechanism of the radular row. LTI therefore combines a force-transmitting role with an articulatory or guiding role. The marginal teeth form a third functional system. Their high aspect ratio, flexible styli and distributed substrate contact are consistent with bending, conforming contact, sweeping and gathering loosened particles; inner marginals participate more strongly in substrate interaction, whereas more lateral marginals are less exposed and more compliant [8,61,62].

The companion FEA likewise found distinct mechanical responses in lateral and marginal teeth [62]. Similar geometry-dependent behaviour was found in earlier taenioglossan FEA studies, where tooth shape and dimensions strongly influenced stress and strain even before material gradients were considered [17,18].

These differences in failure location are examined below.

Time to first structural failure increased in the order LTI < LTII < IMT < MMT < OMT and increased when wet, with the wet-dry difference rising from 0.13 s in LTI to 0.27 s in OMT. Breaking force and loading duration therefore describe different aspects of mechanical performance. At the fixed nominal probe speed, longer loading duration indicates greater imposed probe travel before first failure and is consistent with greater deformation or rearrangement of the tooth–membrane system in rewetted preparations. It cannot, however, be equated directly with greater extension or strain of the individual tooth, because other structures and contacts can also move.

4.3. Material Gradients, Local Reinforcement and Fracture Location

Stiff distal regions and compliant supports have distinct mechanical roles [34–39]. Mineralized chiton and limpet teeth achieve high stiffness and wear resistance [28,30–33], while compliant supports remain important [49,58].

V. turrita follows the same general design principle without heavy bulk mineralization. LTII has the highest measured Young's modulus and hardness, and interacting regions of LTI and the IMT are also locally reinforced, whereas proximal, joint-like or less exposed regions are more compliant [61]. These gradients arise from several mechanisms, including differences in tanning, elemental composition and a calcium-rich superficial coating [61]. Similar thin Ca- or Si-rich coatings have been documented in paludomid, nudibranch, cephalaspidean and cephalopod radulae, where they are interpreted primarily as wear-coping structures [26,43–46]. A reinforced contact zone can therefore coexist with more flexible regions that accommodate bending.

LTI illustrates this combination of stiff and compliant regions. Earlier feeding experiments showed that LTI is mechanically linked to the central tooth through a joint-like

connection that contributes to folding of the radular row [8], and the material-property study identified several joint-like regions as comparatively compliant [61]. In both hydration states, failure occurred at this bridge-like process rather than in the main load-bearing part of LTI. Under wet conditions, the damage remained small and localized, whereas the dry structure crumbled in the same region without a sharp fracture plane. The bridge may therefore function as a mechanically compliant or sacrificial transition that permits movement while protecting the larger tooth body. The difference between localized wet damage and dry crumbling is also compatible with hydration reducing brittle fragmentation, although this interpretation requires direct microstructural comparison of the fractured surfaces.

LTII and the marginal teeth showed a different hydration response. Dry LTII failed at the loaded cusp. After hydration, however, LTII failure occurred variably at the cusp, stylus or basis, indicating that the route to failure became less localized. For the marginal teeth, the failure site shifted: dry marginal teeth failed at the cusp, whereas wet marginals failed at the basis. This wet basal failure agrees with earlier taenioglossan experiments in which flexible marginal teeth frequently failed close to the basis [14]. By contrast, dry cusp failure suggests that reduced compliance can cause damage to remain concentrated near the loaded distal region before large-scale bending develops. These results suggest that local stiffness alone is insufficient to predict failure location.

V. turrita teeth contain a fibrous inner composite below a thin fiber-free surface layer [61]. Fiber architecture and graded interfaces can mitigate and redirect damage [32,53] and reduce mechanical mismatch [47,48].

4.4. Positional Differentiation Within the Marginal Field

Marginal teeth form an integrated functional field [5]. In *V. turrita*, morphology and wear vary across this field [8], as do mechanical properties [61].

IMT, MMT and OMT differed significantly from one another in both hydration states. Breaking force decreased from the inner towards the outer marginal positions, whereas time to first structural failure increased in the opposite direction. The gradient is consistent with their positional differences in morphology, wear and material properties and supports complementary functions within the same tooth row [15,27,36].

4.5. Hydration Controls the Mechanical Failure Pathway and Tooth Function

The native radula operates wet, and its compliant membrane, tooth bases and joint-like regions are part of the mechanism by which teeth change orientation and interact with one another during feeding. Where water can penetrate the matrix, it may plasticize chitin–protein composites and increase deformability; wet chiton radular teeth, for example, show lower hardness and Young's modulus values than dry teeth [30]. The nanoindentation values used for *V. turrita* and for the present FEA were necessarily obtained under dry conditions [61]. These dry values are useful for characterizing spatial stiffness differences, but they do not reproduce the absolute mechanical state in which the radula normally functions. Hydration-dependent compliance may therefore allow greater deformation and load redistribution across the tooth–membrane system before failure, although changes in intrinsic material toughness were not measured here.

Earlier studies of taenioglossan radulae also found that hydrated preparations could resist higher external loads despite greater compliance. Wet teeth can bend or twist more readily; the hydrated membrane permits larger movements of the tooth bases, and some tooth types can gain mechanical support from adjacent rows. These mechanisms redistribute load from the loaded cusp through the stylus, neighboring teeth and membrane and can increase the externally applied force tolerated before final failure [14,56]. In earlier paludomid experiments, broad interlocking teeth could rely on adjacent rows and some-

times failed only when the membrane or a larger tooth row unit ruptured, whereas slender marginal teeth more often deformed independently and failed close to their basis [14].

Attachment geometry also influences the response to hydration. Comparative work on paludomid radulae showed that broad attachment areas can distribute load more evenly, whereas smaller attachment regions allow greater deflection [13,14]. This interpretation is particularly relevant to *V. turrita* because feeding experiments demonstrated extensive folding and unfolding of the membrane, a joint-like LTI-central-tooth connection, and interactions among marginal styli [8]. In hydrated preparations, these connections can contribute to load transfer; reduced compliance in dry preparations may restrict their movement.

The larger duration differences towards OMT and the observed failure sites suggest changes in how the teeth carry load.

4.6. Methodological Limitations of the Experimental Model and FEA

Several aspects of preparation limit direct comparisons with untreated radulae. All specimens underwent graded ethanol/acetone dehydration, CO_2 critical-point drying and epoxy mounting; specimens in the wet treatment were subsequently rewetted with distilled water. Although critical-point drying reduces liquid–gas interface effects during drying, it does not establish that the original distribution of bound water or the native mechanical properties of the chitin–protein material are maintained. Rewetting may not fully restore the native water distribution or polymer interactions, and distilled water does not reproduce the physicochemical conditions present during feeding. Because the salinity and ionic composition of the rewetting medium were not varied, their effects on radular failure resistance remain untested. The influence of hydration on biological materials also depends on their physicochemical environment. For example, theoretical studies of lipid bilayers have described temperature- and pressure-dependent structural transitions, including processes involving hydration [64]. Although these mechanisms are not directly comparable to those of radular teeth, they illustrate the importance of considering environmental conditions when interpreting hydration-dependent material responses. Neither residual water content nor water uptake after rewetting was measured, and freshly dissected, continuously hydrated specimens were not tested. Consequently, the measured forces characterize critical-point-dried and rewetted preparations rather than native in vivo fracture thresholds. Because the initial preparation protocol was identical, the treatment comparison remains informative within these standardized experimental conditions; however, the approximately 26–30% increases measured after rewetting should not be interpreted as quantitative changes expected in living radulae under naturally varying hydration or salinity.

Brief boiling before dissection could also have affected the mechanical response. The properties of chitin–protein composites depend partly on the protein matrix [65], and thermal exposure can alter insect cuticle mechanics [66]. We did not compare boiled and unboiled radulae, so the effect of boiling on *V. turrita* teeth remains unknown. All specimens underwent this treatment, but a common thermal history does not rule out interactions with subsequent rewetting. Comparisons with unboiled, continuously hydrated specimens would help establish how closely the measured forces reflect native conditions.

The companion FEA assumed linear elasticity and a standard 1 N reference load [62]; fracture, membrane mechanics and contacts between teeth were not simulated. Failure sites can therefore be compared qualitatively with modelled stress and strain patterns, but the comparison does not validate fracture predictions or constitute a statistical correlation. The reference load cannot be treated as a physiological or failure force [59]. Here [62], "Rankine strain" denotes the maximum tensile principal strain (the greatest local extension), not the stress-based Rankine failure criterion or a direct prediction of fracture.

Loading duration requires qualification. Because each tooth was subjected to a single continuous loading event at a constant nominal advancement speed of 0.05 mm/s, the measured interval is proportional to nominal probe travel and contains information on the movement imposed before first failure. The loading intervals were on the order of seconds, without repeated loading cycles or a sustained-load hold; accordingly, they do not measure fatigue life or stress relaxation. Although the loading apparatus may be relatively stiff, its compliance relative to the preparation was not independently quantified and probe displacement was not recorded in a separate channel. Nominal probe travel may be distributed among tooth bending, membrane and tissue movement, neighboring-tooth interactions and changes in probe contact. Consequently, a longer loading duration is compatible with greater deformability of the tooth–membrane system but cannot be converted into the local deformation, extension or strain of an individual tooth, or interpreted as a measurement of intrinsic toughness.

4.7. Qualitative Comparison with the Companion FEA Study

The companion FEA [62] provides a qualitative comparison with the observed failure sites. It modelled LTI, LTII, IMT and OMT, but not MMT, using heterogeneous elastic properties based on dry nanoindentation data and homogeneous reference moduli of 8.5 and 19 GPa.

The breaking force experiments, in contrast to the individual-tooth FEA, retained the three-dimensional radular curvature, relative tooth orientation and potential tooth-to-tooth support. This preserves important aspects of the spatial organization observed during feeding [8], although the imposed shear load is an experimental challenge rather than a direct measurement of in vivo loading.

The experimentally observed failure patterns show some qualitative anatomical consistencies with the companion FEA. Dry LTII failed at the cusp, broadly consistent with the localized cusp-dominated mechanical response predicted for the lateral teeth. Rewetted marginal teeth were observed to fail at the basis, in the general region towards which the marginal-tooth models showed extended stylus deformation and bending-related strain. However, those models were based on dry material properties and did not simulate hydration-dependent changes; spatial proximity should therefore not be interpreted as confirmation of a particular fracture mechanism. Conversely, the observed dry marginal cusp failure did not correspond to the principal proximal bending-related strain region, while wet LTII displayed variable failure locations at the cusp, stylus or basis rather than a unique anatomical correspondence.

The LTI bridge-like process illustrates a further limitation of comparing these two datasets. The experimentally vulnerable region lies at a joint-associated connection with the central tooth that contributes to folding of the tooth row [8]. A simplified model of an individual tooth cannot reproduce the contact and load transfer occurring at that tooth-to-tooth connection. Failure at this site therefore neither confirms nor refutes the individual-tooth FEA; it instead points to a structural feature that future multi-tooth, contact-based models would need to represent.

Overall, the FEA comparison supports discussion of plausible regional deformation patterns and functional specialization, but it is not an independent quantitative validation of the breaking force measurements. A direct predictive comparison would require matched loading and boundary conditions, appropriate hydrated material properties, explicit inter-tooth and membrane contacts, and a fracture or damage model. The distinction between physiological feeding forces and experimentally determined structural failure forces also remains essential [7,12,14].

Hydration might also modify crack propagation through crack arrest, deflection or branching, potentially shifting damage to other tooth regions. These mechanisms remain hypothetical because crack development was not monitored during loading. Future studies could combine dye-assisted visualization of microcracks with local stress-field analyses and material-specific estimates of critical crack length to test whether these processes contribute to the observed hydration-dependent failure patterns.

4.8. Wear Resistance, Fracture Resistance and Renewal

Resistance to abrasion and resistance to fracture depend on partly different properties. Hardness, depending on the presence of mineral phases and surface coatings, can reduce abrasion, whereas resistance to catastrophic structural failure may depend more strongly on geometry, fiber architecture, compliant transition zones and load sharing. In highly mineralized chiton and limpet teeth, bulk reinforcement and organized nanostructure support extreme wear performance [29–31,33]. In *V. turrita*, by contrast, targeted local reinforcement appears to be combined with substantial compliance. The calcium-rich coating is concentrated at mechanically relevant regions and is well suited to limiting surface damage, while the underlying fibrous composite and softer tooth regions may control bending and crack propagation [61]. This is consistent with mineral enrichment previously described in other neritid teeth, including *Nerita atramentosa* [67].

The distinction between wear and fracture is nevertheless not absolute. In *V. turrita*, abrasive feeding experiments documented a sequence from scratches to fractures and spalling, indicating that repeated surface damage can eventually develop into structural loss [8,63]. Similar relations between wear pattern, architecture and local mechanical properties have been documented in other molluscan radulae [26,51–53]. Breaking force tests complement wear studies by measuring failure under a single imposed load rather than damage accumulated during repeated contacts.

The radula is also a continuously renewed organ. Teeth are produced in the posterior radular sac, mature as they move towards the working zone and are ultimately lost or degraded after service [54,55]. Individual teeth need to remain functional only until they are replaced. Controlled wear, local fracture, compliant deformation and collective tooth support may therefore represent complementary strategies that prevent catastrophic failure of the entire feeding apparatus. Such localized fracture could help confine damage when teeth encounter feeding substrates of different roughness or mechanical resistance, although whether this represents a substrate-specific adaptation remains to be tested.

In brackish mangrove and riverine habitats, *V. turrita* uses its differentiated radula to graze on submerged surfaces [8,60]. The relatively high failure resistance of LTII is consistent with a scraping role, whereas more compliant marginal teeth may accommodate surface irregularities and help gather loosened particles. Hydration-dependent compliance could help limit damage during such contacts and maintain feeding function between successive tooth replacements. These are functional implications rather than directly demonstrated ecological benefits: the present tests measured failure under imposed loads, not the forces generated during natural feeding.

4.9. A Hierarchical Model of Radular Mechanical Specialization

Several levels of organization contribute to radular performance: organ kinematics set loading [1,6,10]; tooth row architecture governs engagement and load sharing [5,8,9,13,14]; geometry and stiffness govern tooth response [17,18,34,36,62]; microstructure contributes to wear and fracture resistance [32,41,43–45,53,61]; and hydration controls expressed compliance [14,56].

The five tooth types differed in the loads they could withstand and in how they failed. LTII is specialized for localized substrate interaction and concentrated force transmission; LTI contributes to substrate loading but also forms part of the folding and guiding mechanism of the tooth row; and the marginal teeth are geometrically configured for progressively greater compliance, surface conformity and particle-handling ability [8,61,62]. These experiments indicate that tooth function cannot be inferred from morphology or dry material properties alone.

From a biomimetic perspective, a combination of reinforced contact regions and compliant attachments may provide a useful principle for small scraping or particle-handling devices operating in water. The observed dependence on hydration suggests that such designs should be evaluated under their intended wet operating conditions rather than solely from dry material properties [29,39]. This proposed application remains to be tested in engineered systems.

5. Conclusions

Vittina turrita has a functionally differentiated, hydration-dependent radula. Breaking force followed LTII > LTI > IMT > MMT > OMT, whereas time to first structural failure increased from LTI to OMT. Hydration increased both breaking force and loading duration and changed failure location: LTI damage remained joint-associated, LTII failure became more variable, and marginal teeth shifted from cusp to basal failure. Taken together, the results suggest that geometry and material differences contribute to failure behaviour, while rewetting changes the response of the prepared tooth–membrane system.

Supplementary Materials: The following supporting information can be downloaded at https://www.mdpi.com/article/10.3390/ani16233807/s1: Supplementary Tables S1–S7 provide descriptive statistics, distributional tests, GEE results, post hoc comparisons and qualitative failure patterns. Supplementary Data S1 contains the 3000 individual tooth measurements (Excel workbook).

Author Contributions: Conceptualization, W.K. and S.N.G.; methodology, W.K. and S.N.G.; interpretation, W.K.; formal analysis. All authors have read and agreed to the published version of the manuscript.

Funding: This research was funded by the Deutsche Forschungsgemeinschaft (DFG), grant number 470833544 (to W.K.).

Institutional Review Board Statement: Ethical review and approval were not required for this study because the experimental animals, *Vittina turrita* (Gastropoda), are invertebrates not covered by the approval requirements of Directive 2010/63/EU or the German Animal Welfare Act (TierSchG, § 8). Specimens were obtained from a commercial aquarium supplier, and mechanical experiments were performed on dissected radular preparations after the animals had been killed, as described in the Materials and Methods. Animals were killed solely to obtain radulae for subsequent ex vivo mechanical testing. According to Section 7(2) of the German Animal Welfare Act (Tierschutzgesetz), killing animals exclusively for the scientific examination of their organs or tissues is not classified as an animal experiment. Furthermore, the approval requirement under Section 8(1) applies to experiments involving vertebrates and cephalopods. Therefore, formal ethical approval was not required for the present study.

Informed Consent Statement: Not applicable.

Data Availability Statement: Individual tooth-level breaking force and time-to-failure measurements from all 3000 tests, including specimen identity and tooth category, are provided in Supplementary Data S1 (Excel workbook). Descriptive statistics, model results and qualitative failure descriptions are provided in Supplementary Tables S1–S7.

Acknowledgments: We thank Elke Woelken (University of Hamburg) for assistance with scanning electron microscopy. OpenAI's ChatGPT GPT-6 Thinkingwas used to assist with language editing.

The authors reviewed the scientific content, references and final text and take responsibility for the manuscript.

Conflicts of Interest: The authors declare no conflict of interest.

References

1. Guralnick, R.; Smith, K. Historical and biomechanical analysis of integration and dissociation in molluscan feeding, with special emphasis on the true limpets (Patellogastropoda: Gastropoda). *J. Morphol.* **1999**, *241*, 175–195. [CrossRef]
2. Mackenstedt, U.; Märkel, K. Radular structure and function. In *The Biology of Terrestrial Molluscs*; Barker, G.M., Ed.; CABI Publishing: Oxon, UK, 2001; pp. 213–236.
3. Haszprunar, G.; Götting, K.J. Mollusca, Weichtiere. In *Spezielle Zoologie. Teil 1. Einzeller und Wirbellose Tiere*; Westheide, W., Rieger, G., Eds.; Springer: Berlin, Germany, 2007.
4. Hickman, C.S. Gastropod radulae and the assessment of form in evolutionary paleontology. *Paleobiology* **1980**, *6*, 276–294. [CrossRef]
5. Hickman, C.S. Implications of radular tooth-row functional integration for archaeogastropod systematics. *Malacologia* **1984**, *25*, 143–160.
6. Scheel, C.; Gorb, S.N.; Glaubrecht, M.; Krings, W. Not just scratching the surface: Distinct radular motion patterns in Mollusca. *Biol. Open* **2020**, *9*, bio055699. [CrossRef] [PubMed]
7. Krings, W.; Faust, T.; Kovalev, A.; Neiber, M.T.; Glaubrecht, M.; Gorb, S.N. In slow motion: Radula motion pattern and forces exerted to the substrate in the land snail *Cornu aspersum* (Mollusca, Gastropoda) during feeding. *R. Soc. Open Sci.* **2019**, *6*, 190222. [CrossRef] [PubMed]
8. Krings, W.; Hempel, C.; Siemers, L.; Neiber, M.T.; Gorb, S.N. Feeding experiments on *Vittina turrita* (Mollusca, Gastropoda, Neritidae) reveal tooth contact areas and bent radular shape during foraging. *Sci. Rep.* **2021**, *11*, 9556. [CrossRef] [PubMed]
9. Krings, W.; Karabacak, H.; Gorb, S.N. From the knitting shop: The first physical and dynamic model of the taenioglossan radula (Mollusca: Gastropoda) aids in unravelling functional principles of the radular morphology. *J. R. Soc. Interface* **2021**, *18*, 20210377. [CrossRef] [PubMed]
10. Neustadter, D.M.; Drushel, R.F.; Chiel, H.J. Kinematics of the buccal mass during swallowing based on magnetic resonance imaging in intact, behaving *Aplysia californica*. *J. Exp. Biol.* **2002**, *205*, 939–958. [CrossRef] [PubMed]
11. Montroni, D.; Zhang, X.; Leonard, J.; Kaya, M.; Amemiya, C.; Falini, G.; Rolandi, M. Structural characterization of the buccal mass of *Ariolimax californicus* (Gastropoda; Stylommatophora). *PLoS ONE* **2019**, *14*, e0212249. [CrossRef] [PubMed]
12. Krings, W.; Neumann, C.; Neiber, M.T.; Kovalev, A.; Gorb, S.N. Radular force performance of stylommatophoran gastropods (Mollusca) with distinct body masses. *Sci. Rep.* **2021**, *11*, 10560. [CrossRef] [PubMed]
13. Krings, W.; Brütt, J.-O.; Gorb, S.N.; Glaubrecht, M. Tightening it up: Diversity of the chitin anchorage of radular teeth in paludomid freshwater gastropods. *Malacologia* **2020**, *63*, 77–94. [CrossRef]
14. Krings, W.; Kovalev, A.; Gorb, S.N. Collective effect of damage prevention in taenioglossan radular teeth is related to the ecological niche in Paludomidae (Gastropoda: Cerithioidea). *Acta Biomater.* **2021**, *135*, 458–472. [CrossRef] [PubMed]
15. Hawkins, S.J.; Watson, D.C.; Hill, A.S.; Harding, S.P.; Kyriakides, M.A.; Hutchinson, S.; Norton, T.A. A comparison of feeding mechanisms in microphagous, herbivorous, intertidal, prosobranchs in relation to resource partitioning. *J. Molluscan Stud.* **1989**, *55*, 151–165. [CrossRef]
16. Padilla, D.K. Form and function of radular teeth of herbivorous molluscs: Focus on the future. *Am. Malacol. Bull.* **2003**, *18*, 163–168.
17. Krings, W.; Marcé-Nogué, J.; Karabacak, H.; Glaubrecht, M.; Gorb, S.N. Finite element analysis of individual taenioglossan radular teeth (Mollusca). *Acta Biomater.* **2020**, *115*, 317–332. [CrossRef] [PubMed]
18. Krings, W.; Marcé-Nogué, J.; Gorb, S.N. Finite element analysis relating shape, material properties, and dimensions of taenioglossan radular teeth with trophic specialisations in Paludomidae (Gastropoda). *Sci. Rep.* **2021**, *11*, 22775. [CrossRef] [PubMed]
19. Walsby, J.R. Feeding and the radula in the marine pulmonate limpet *Trimusculus reticulatus*. *Veliger* **1975**, *18*, 139–145.
20. Steneck, R.S.; Watling, L. Feeding capabilities and limitation of herbivorous molluscs: A functional group approach. *Mar. Biol.* **1982**, *68*, 299–319. [CrossRef]
21. Blinn, W.; Truitt, R.E.; Pickart, A. Feeding ecology and radular morphology of the freshwater limpet *Ferrissia fragilis*. *J. N. Am. Benthol. Soc.* **1989**, *8*, 237–242. [CrossRef] [PubMed]
22. Padilla, D.K. Inducible phenotypic plasticity of the radula in *Lacuna* (Gastropoda: Littorinidae). *Veliger* **1998**, *41*, 201–204.
23. Padilla, D.K. Food and environmental cues trigger an inducible offense. *Evol. Ecol. Res.* **2001**, *3*, 15–25.
24. Duda, T.F.; Kohn, A.J.; Palumbi, S.R. Origins of diverse feeding ecologies within *Conus*, a genus of venomous marine gastropods. *Biol. J. Linn. Soc.* **2001**, *73*, 391–409. [CrossRef]

25. Krings, W. Trophic Specialization of Paludomid Gastropods from 'Ancient' Lake Tanganyika Reflected by Radular Tooth Morphologies and Material Properties. Ph.D Thesis, University of Hamburg, Hamburg, Germany, 2020.
26. Hackethal, S.; Schulz-Kornas, E.; Gorb, S.N.; Krings, W. Wear patterns of radular teeth in *Loligo vulgaris* (Cephalopoda; Mollusca) are related to their structure and mechanical properties. *Interface Focus* **2024**, *14*, 20230082. [CrossRef] [PubMed]
27. Krings, W.; Hausdorf, B.; Gorb, S.N. Ecomechanics of molluscs' radula. *Biointerphases* **2026**, *21*, 011001. [CrossRef] [PubMed]
28. van der Wal, P. Structural and material design of mature mineralized radula teeth of *Patella vulgata* (Gastropoda). *J. Ultrastruct. Mol. Struct. Res.* **1989**, *102*, 147–161. [CrossRef]
29. van der Wal, P.; Giesen, H.J.; Videler, J.J. Radular teeth as models for the improvement of industrial cutting devices. *Mater. Sci. Eng. C* **1999**, *7*, 129–142. [CrossRef]
30. Weaver, J.C.; Wang, Q.; Miserez, A.; Tantuccio, A.; Stromberg, R.; Bozhilov, K.N.; Maxwell, P.; Nay, R.; Heier, S.T.; DiMasi, E. Analysis of an ultra hard magnetic biomineral in chiton radular teeth. *Mater. Today* **2010**, *13*, 42–52. [CrossRef]
31. Lu, D.; Barber, A.H. Optimized nanoscale composite behaviour in limpet teeth. *J. R. Soc. Interface* **2012**, *9*, 1318–1324. [CrossRef] [PubMed]
32. Grunenfelder, L.K.; de Obaldia, E.E.; Wang, Q.; Li, D.; Weden, B.; Salinas, C.; Wuhrer, R.; Zavattieri, P.; Kisailus, D. Biomineralization: Stress and damage mitigation from oriented nanostructures within the radular teeth of *Cryptochiton stelleri*. *Adv. Funct. Mater.* **2014**, *24*, 6093–6104. [CrossRef]
33. Barber, A.H.; Lu, D.; Pugno, N.M. Extreme strength observed in limpet teeth. *J. R. Soc. Interface* **2015**, *12*, 20141326. [CrossRef] [PubMed]
34. Krings, W.; Kovalev, A.; Glaubrecht, M.; Gorb, S.N. Differences in the Young modulus and hardness reflect different functions of teeth within the taenioglossan radula of gastropods. *Zoology* **2019**, *137*, 125713. [CrossRef] [PubMed]
35. Krings, W.; Neiber, M.T.; Kovalev, A.; Gorb, S.N.; Glaubrecht, M. Trophic specialisation reflected by radular tooth material properties in an 'ancient' Lake Tanganyikan gastropod species flock. *BMC Ecol. Evol.* **2021**, *21*, 35. [CrossRef] [PubMed]
36. Gorb, S.N.; Krings, W. Mechanical property gradients of taenioglossan radular teeth are associated with specific function and ecological niche in Paludomidae (Gastropoda: Mollusca). *Acta Biomater.* **2021**, *134*, 513–530. [CrossRef] [PubMed]
37. Krings, W.; Matsumura, Y.; Brütt, J.-O.; Gorb, S.N. Material gradients in gastropod radulae and their biomechanical significance: A combined approach on the paludomid *Lavigeria grandis*. *Sci. Nat.* **2022**, *109*, 52. [CrossRef] [PubMed]
38. Krings, W.; Gorb, S.N. Diversity of mineral systems, material compositions and mechanical properties in molluscan radulae. In *Metals and Their Functional Role in the Structures of Invertebrates*; Lehnert, M.S., Ed.; Springer: Cham, Switzerland, 2024; pp. 173–214.
39. Krings, W.; Gorb, S.N. Performance of biological food processing interfaces: Perspectives on the science of mollusc radula. *Biointerphases* **2024**, *19*, 030801. [CrossRef] [PubMed]
40. Degtyar, E.; Harrington, M.J.; Politi, Y.; Fratzl, P. The mechanical role of metal ions in biogenic protein-based materials. *Angew. Chem. Int. Ed.* **2014**, *53*, 12026–12044. [CrossRef] [PubMed]
41. Krings, W.; Brütt, J.-O.; Gorb, S.N. Elemental analyses reveal distinct mineralization patterns in radular teeth of various molluscan taxa. *Sci. Rep.* **2022**, *12*, 7499. [CrossRef] [PubMed]
42. Krings, W.; Brütt, J.-O.; Gorb, S.N. Ontogeny of the elemental composition and the biomechanics of radular teeth in the chiton *Lepidochitona cinerea*. *Front. Zool.* **2022**, *19*, 19. [CrossRef] [PubMed]
43. Krings, W.; Wägele, H.; Neumann, C.; Gorb, S.N. Coping with abrasive food: Diverging composition of radular teeth in two Porifera-consuming nudibranch species (Mollusca, Gastropoda). *J. R. Soc. Interface* **2023**, *20*, 20220927. [CrossRef] [PubMed]
44. Krings, W.; Neumann, C.; Gorb, S.N.; Koehnsen, A.; Wägele, H. Elemental composition and material properties of radular teeth in the heterobranch snail *Gastropteron rubrum* (Mollusca, Gastropoda, Cephalaspidea) foraging on hard organisms. *Ecol. Evol.* **2023**, *13*, e10332. [CrossRef] [PubMed]
45. Krings, W.; Gorb, S.N.; Neumann, C.; Wägele, H. Radular tooth coating in members of Dendronotidae and Flabellinidae (Nudibranchia, Gastropoda, Mollusca). *J. Morphol.* **2024**, *285*, e21773. [CrossRef] [PubMed]
46. Krings, W.; Gorb, S.N. Foraging on sand particles: Coatings of soft radular teeth (Paludomidae, Gastropoda, Mollusca). *Invertebr. Biol.* **2023**, *142*, e12410. [CrossRef]
47. Miserez, A.; Schneberk, T.; Sun, C.; Zok, F.W.; Waite, J.H. The transition from stiff to compliant materials in squid beaks. *Science* **2008**, *319*, 1816–1819. [CrossRef] [PubMed]
48. Liu, Z.Q.; Zhu, Y.K.; Jiao, D.; Weng, Z.Y.; Zhang, Z.F.; Ritchie, R.O. Enhanced protective role in materials with gradient structural orientations: Lessons from nature. *Acta Biomater.* **2016**, *44*, 31–40. [CrossRef] [PubMed]
49. Pohl, A.; Herrera, S.A.; Restrepo, D.; Negishi, R.; Jung, J.-Y.; Salinas, C.; Wuhrer, R.; Yoshino, T.; McKittrick, J.; Arakaki, A.; et al. Radular stylus of *Cryptochiton stelleri*: A multifunctional lightweight and flexible fiber-reinforced composite. *J. Mech. Behav. Biomed. Mater.* **2020**, *111*, 103991. [CrossRef] [PubMed]
50. Runham, N.W.; Thornton, P.R. Mechanical wear of the gastropod radula: A scanning electron microscope study. *J. Zool.* **1967**, *153*, 445–452. [CrossRef]

51. Shaw, J.A.; Macey, D.J.; Brooker, L.R.; Clode, P.L. Tooth use and wear in three iron-biomineralizing mollusc species. *Biol. Bull.* **2010**, *218*, 132–144. [CrossRef] [PubMed]
52. Krings, W.; Gorb, S.N. Substrate roughness induced wear pattern in gastropod radulae. *Biotribology* **2021**, *26*, 100164. [CrossRef]
53. Krings, W.; Brütt, J.-O.; Gorb, S.N. Micro-cracks and micro-fractures reveal radular tooth architecture and its functional significance in the paludomid gastropod *Lavigeria grandis*. *Philos. Trans. R. Soc. A* **2022**, *380*, 20210335. [CrossRef] [PubMed]
54. Mackenstedt, U.; Märkel, K. Experimental and comparative morphology of radula renewal in pulmonates (Mollusca, Gastropoda). *Zoomorphology* **1987**, *107*, 209–239. [CrossRef]
55. Shaw, J.A.; Brooker, L.R.; Macey, D.J. Radula tooth turnover in the chiton, *Acanthopleura hirtosa* (Blainville, 1825) (Mollusca: Polyplacophora). *Molluscan Res.* **2002**, *22*, 93–99.
56. Krings, W.; Kovalev, A.; Gorb, S.N. Influence of water content on mechanical behaviour of gastropod taenioglossan radulae. *Proc. R. Soc. B* **2021**, *288*, 20203173. [CrossRef] [PubMed]
57. Gadomski, A. Stretched exponential kinetics of the pressure induced hydration of model lipid membranes. A possible scenario. *J. Phys. II Fr.* **1996**, *6*, 1537–1546. [CrossRef]
58. Herrera, S.A.; Grunenfelder, L.; Escobar, E.; Wang, Q.; Salinas, C.; Yaraghi, N.; Geiger, J.; Wuhrer, R.; Zavattieri, P.; Kisailus, D. Stylus support structure and function of radular teeth in *Cryptochiton stelleri*. In Proceedings of the 20th International Conference on Composite Materials, Copenhagen, Denmark, 19–24 July 2015.
59. Dumont, E.R.; Grosse, I.R.; Slater, G.J. Requirements for comparing the performance of finite element models of biological structures. *J. Theor. Biol.* **2009**, *256*, 96–103. [CrossRef] [PubMed]
60. Hristov, K.K. Observations on Neritina turrita (Gmelin 1791) breeding behaviour in laboratory conditions. *Indian J. Pure Appl. Biosci.* **2020**, *8*, 1–10. [CrossRef]
61. Krings, W.; Schulz-Kornas, E.; Gorb, S.N. Wear-coping mechanisms and functional morphology of the radular teeth of *Vittina turrita* (Neritimorpha, Gastropoda). *J. R. Soc. Interface* **2025**, *22*, 20250016. [CrossRef] [PubMed]
62. Krings, W.; Gorb, S.N.; Schulz-Kornas, E.; Marcé-Nogué, J. Effects of the geometry and material stiffness distribution on stress and strain in *Vittina turrita* radular teeth. *J. Comp. Physiol. A. in press*.
63. Krings, W.; Gorb, S.N.; Schulz-Kornas, E. Dental microwear texture analysis on radular teeth. *Adv. Mater. Interfaces* **2026**, *13*, e70665. [CrossRef]
64. Gadomski, A.; Łuczka, J. Kinetics of temperature or pressure field induced phase transformation in lipid bilayers. *Acta Phys. Pol. B* **1997**, *28*, 1827–1842.
65. Montroni, D.; Sparla, F.; Fermani, S.; Falini, G. Influence of proteins on mechanical properties of a natural chitin-protein composite. *Acta Biomater.* **2021**, *120*, 81–90. [CrossRef] [PubMed]
66. Kuhn, H.F.; Müssig, J.; Dirks, J.-H. Dynamic mechanical analysis reveals reversible thermal effects in insect tibial cuticle. *J. Mech. Behav. Biomed. Mater.* **2026**, *179*, 107450. [CrossRef] [PubMed]
67. Macey, D.J.; Brooker, L.R.; Cameron, V. Mineralisation in the teeth of the gastropod mollusc *Nerita atramentosa*. *Molluscan Res.* **1997**, *18*, 33–41. [CrossRef]

Disclaimer/Publisher's Note: The statements, opinions and data contained in all publications are solely those of the individual author(s) and contributor(s) and not of MDPI and/or the editor(s). MDPI and/or the editor(s) disclaim responsibility for any injury to people or property resulting from any ideas, methods, instructions or products referred to in the content.